SPATIAL ECONOMIC ANALYSIS
https://doi.org/10.1080/17421772.2022.2096917



# The local costs of global climate change: spatial GDP downscaling under different climate scenarios

Massimiliano Rizzati [a], Gabriele Standardi [b,c], Gianni Guastella [a,d], Ramiro Parrado [b,c], Francesco Bosello [b,c] and Stefano Pareglio [a,d]

**ABSTRACT**

We present a tractable methodology to estimate climate change costs at a 1 × 1 km grid resolution. Climate change costs are obtained as projected gross domestic product (GDP) changes, under different global shared socio-economic pathway–representative concentration pathway (SSP-RCP) scenarios, from a regional (multiple European NUTS levels) version of the Intertemporal Computable Equilibrium System (ICES) model. Local costs are obtained by downscaling projected GDP according to urbanized area estimated by a grid-level model that accounts for fixed effects, such as population and location, and spatially clustered random effects at multiple hierarchical administrative levels. We produce a grid-level dataset of climate change economic impacts under different scenarios that can be used to compare the cost – in terms of GDP loss – of no adaptation and the benefits of investing in local adaptation.

**KEYWORDS**

statistical downscaling, linear mixed models, climate change, adaptation costs, urban area projections

**JEL** C15, Q54, R14

**HISTORY** Received 6 May 2021; in revised form 17 June 2022

## 1. INTRODUCTION

The temperature rise caused and magnified by anthropogenic activity might reach, in the next decades, 3°C in 2050 and even more after 2100, according to the Intergovernmental Panel on Climate Change (IPCC) (Masson-Delmotte et al., 2018). The different pathways will exhibit profoundly diversified effects on people and income levels through the channels of both physical and transition risks, especially in the absence of adaptation measures. The availability of informative and detailed data at different spatial scales is of paramount importance in developing proper policy actions to curb greenhouse gas (GHG) emissions and in strengthening adaptation capacity. There are also profound economic consequences, as the loss of gross domestic product (GDP) due to missed adaptation measures might be severe and heterogeneously distributed in space. Therefore, frameworks to project and map these costs across different scenarios are needed.

The mitigation processes available to address the emission levels and their potential impact on climate change often display a global dimension. Accordingly, most models developed to assess

**CONTACT** Massimiliano Rizzati Massimiliano.rizzati@feem.it
[a] Fondazione Eni Enrico Mattei Sede di Milano, Milan, Italy
[b] RFF-CMCC EIEE, Venice, Italy
[c] Ca' Foscari University of Venice, Venice, Italy
[d] Università Cattolica del Sacro Cuore, Brescia, Italy

these impacts work at a global scale (Gambhir et al., 2017). Nonetheless, the extension to smaller scale outputs is an essential objective of the climate change impacts literature (Jones & O'Neill, 2013) because of the spatial and temporal heterogeneity in climate impacts' distribution and the often-local scope of adaptation countermeasures. Climate change impacts are likely to vary in accordance with location and industry mix (Rohat, 2018; Farmer et al., 2015; Carleton & Hsiang, 2016), and models that translate climate into economic impact should vary as well.

The Inter-temporal Computable Equilibrium System (ICES) is a global, top-down recursive-dynamic, multi-sector and multi-country computable general equilibrium (CGE) model based upon the Global Trade Analysis Project (GTAP) database (Narayanan et al., 2012), which takes into account linkages between economic activities, energy use and emissions (Parrado & De Cian, 2014). The ICES model was employed to assess the impacts of climate change in Europe as part of the toolkit used in the CO-designing the Assessment of Climate CHange costs (COACCH) project. For the project's purposes, the model spatial detail has been tailored to regions using a combination of the European NUTS[1] levels and following the methodology of Bosello and Standardi (2018). Refining the model's spatial resolution constitutes an effort to provide more detailed information at the sub-country level for policy design and implementation. This particular feature makes it possible to improve the integration of climate change impacts in the CGE framework, since physical impacts of climate change are projected by process-based biophysical models, which produce information at a higher granularity than the national level.

Further spatial downscaling from the regional to the urban level is still highly important, especially in the case of climate impacts characterized by substantial spatial heterogeneity, such as sea-level rise, coastal storms and heatwaves (Jones & O'Neill, 2016). We propose a procedure for the statistical downscaling of GDP projections produced by the regional ICES model at the 1 km resolution grid level. The 1 km grid represents the finest resolution made available by the Geographical Information System of the European Commission (GISCO-Eurostat). By comparing the downscaled GDP across different scenarios, it is possible to estimate the costs induced by climate change against alternative adaptation approaches at the grid level and, by aggregation, at the city or village level.

Statistical downscaling is a consolidated approach used to disaggregate information through the application of real-life and model-generated weights (Murakami & Yamagata, 2019). Complex algorithms can be applied to guide the choice of the downscaling weights, but the size of data stemming from the required resolutions might limit the application of such approaches from a technical standpoint (Yamagata & Seya, 2019). As a result, using high-resolution grids for the downscaling represents an obstacle to the application of complex – and, hence, more precise – algorithms, such as those that are parametrized (Gao, 2017).

In this work, we propose a simple yet reliable and computationally feasible procedure even for high-resolution grids. The downscaling approach uses the urbanized area to map the spatial distribution of current GDP, a standard method in the literature (Murakami & Yamagata, 2019). A multilevel model linking the urbanized area to population and grid-specific geographical characteristics is used to forecast the urbanized area according to the demographic changes of the scenario under consideration. The forecast urbanized area is then used to map the spatial distribution of projected GDP, and the GDP change associated with a specific scenario, which is the measure of climate change economic costs, is computed accordingly.

Compared with modelling approaches that take into account the spatial connectivity structures implicit in the data (Murakami & Yamagata, 2019), whose estimation may become unfeasible with large datasets (Yamagata & Seya, 2019), the proposed methodology is computationally feasible in standard machines even with many observations. Downscaling of future GDP projections, in fact, requires a projection of the background variable, that is, the urbanized area. This variable should be considered endogenous and, hence, conditional on the values of the selected

scenario. Such a downscaling approach with endogenous background variables requires the estimation of a grid-level statistical model. In the proposed approach, the estimation is carried out by using mixed models. The variability in the observed grid-level urbanization is linked to a fixed part, a combination of population and geographical characteristics such as the distances from important urbanization hotspots, and a random part, the sum of multiple random effects at different and hierarchically organized spatial levels. The presence of multiple random effects at different spatial levels makes it possible to remove unobserved spatial heterogeneity from the fixed part, thus improving the model's predictive capacity without compromising its feasibility.

The remainder of the paper is structured as follows. Section 2 provides some context by summarizing the literature on related topics. Section 3 illustrates the downscaling approach in detail. Section 4 presents the data used to calibrate the downscaling procedure and their sources, as well as the starting projections from the ICES model. Section 5 presents and discusses the estimation results for the model and provides some robustness and validation tests. Finally, Section 6 describes the resulting datasets and proposes this approach as a valid starting point for more complex analyses of the spatial distribution of climate impacts.

## 2. RELATED LITERATURE

Downscaling approaches refer to information-guided disaggregation of data towards a unit of reference of lower spatial resolution. These approaches were developed to bridge the results provided by climate and weather models and the needs of impact evaluators (Wilby & Wigley, 1997). At the foundation of the methodology, there is the distribution of information through weights, often taken as exogenous. In consideration of the growing need to use downscaling approaches with projected data, the weights should be considered endogenous and projected as well. While this review focuses on works that downscale GDP, it also necessarily considers studies that downscale population and urbanized areas, which are often used as weights for the former.

Alongside the development of models and projections related to climate change, downscaling approaches have been extended to target relevant socio-economic variables. The latter often come from top-down aggregated models, or aggregate statistics gathered from national or international institutions, and are available predominantly at the national or regional level (Swan & Ugursal, 2009). Aided by the increasing availability of information from remote-sensing platforms, many studies have also targeted other applications, such as emissions, land use, land cover (Fang & Jawitz, 2018) and, as in the scope of this work, GDP levels (Murakami & Yamagata, 2019).

In what is considered one of the first seminal works in this literature, Gaffin et al. (2004) propose a linear downscaling of global population and GDP until 2100 for the Special Report on Emissions Scenarios (SRES) data A1, A2, B1 and B2 at 0.25 × 0.25° resolution. Their methodology downscales SRES data at the national level through country data and scenario growth rates, and then to the grid level, by using the projections of the Gridded Population of the World data (GPW) (CIESIN, 2004) as weights. As limitations, the authors report implausibly high growth rates, a discontinuity of the projection algorithm, and an assumption of independence between population and GDP levels. van Vuuren et al. (2007) apply an external-input-based downscaling for population and a convergence-based downscaling for GDP and emissions by the IPCC-SRES scenarios; first at the country level (using national data projections as weights), and then at a grid level of 0.5 × 0.5° (using GPW data as weights for population, and then multiplying GDP per capita projections). The authors acknowledge that they do not consider structural relationships between variables and potentially related variables such as infrastructure, education or urbanization. Grübler et al. (2007) downscale population and GDP from 1990

to 2100, as obtained from the A2, B1 and B2 SRES scenarios, to the national level and then to a 0.5° grid resolution. The weights used are the GPW, the ESRI Digital Chart of the World (DCW,, n.d.) and measurements of night-time lights from the National Oceanic and Atmospheric Administration (NOAA) (Elvidge et al., 1997). They employ a two-step approach: a first estimate of the mathematical equation for GDP growth and income (GDP per capita) and then an optimization procedure to reconcile regional deviations from the country's total. Among the limitations of that procedure, the authors report the non-availability of starting data, inconsistencies in available data and non-addressing uncertainty.

Bengtsson et al. (2006) propose a trend extrapolation approach to downscale population data in the 1990–2100 time frame from SRES scenarios, accounting for the separation of urban and rural areas in 0.5° grids and using the LandScan land cover data (Dobson et al., 2000) to distribute the data at the grid level. The authors highlight the heterogeneous definitions of urban populations among countries as a limitation and adopt a constant urbanization ratio. In the case of population, referring to more specific demographic data is sometimes advocated, although their availability is often questioned (Yamagata et al., 2015).

Asadoorian (2008) simulates population and emissions to 2100 by employing a conditional beta distribution with parameters calibrated on macroeconomic variables to a 1° resolution, fitted with a maximum likelihood estimate. Without the same theoretical underpinnings, these results seem to match the predictions of New Economic Geography models (Forslid & Ottaviano, 2003). Nam and Reilly (2013) downscale population density starting from the NASA Socioeconomic Data and Application Center (SEDAC) for the period 1990–2015, to a 0.25° grid with a rank-size rule-based approach to estimate city size and guiding the distribution with variables such as natural endowments, industrial structure, development stage, political centrality and region-specific fixed effects.

Jones and O'Neill (2013) propose a gravity approach to downscale the US population in the A2 and B2 SRES scenarios to a 1/8° grid. Their approach builds on a population potential model with free parameters calibrated with historical values and includes multiple scales of spatial analysis and urban and rural separation. In a different paper, the same authors propose an analysis at the global level (Jones & O'Neill, 2016), adopting a parametrized downscaled gravity approach for urban and non-urban areas that distributes population from all five shared socio-economic pathways (SSPs) (O'Neill et al., 2015; Riahi et al., 2017). They report that gravity-based approaches might result in non-zero population values even in unrealistically inhabited areas. McKee et al. (2015) look at the US population for 2030 and 2050 and apply a locally adaptive spatial interpolation technique and dasymetric modelling, using as a weight a potential development coefficient based on land cover, slopes, population, roads and distance to cities at a 1-arc-sec resolution. This latter work, however, does not address climate change, land cover change and migration.

Yamagata et al. (2015) apply a multi-model approach to Japanese population projections that also compares different downscaling methods, such as constant-share, share of growth, log-linear trend extrapolation methods, time-series methods (ARIMA), to estimate residential electricity at the 1 $km^2$ resolution. They evaluate the different approaches in terms of $R^2$ and root mean square error (RMSE) against actual data from the Tokyo area. As a limitation, they report the need to consider auxiliary information.

Taking the global population as a starting point and the GPW as weights, Fujimori et al. (2017) downscale it with a rank-size rule. Given the population, the approach distributes GDP and emissions to a 0.5° grid that takes into consideration physical constraints such as mountains, water bodies and urban sprawl. They highlight how the emission allocation could need additional spatial drivers. Kummu et al. (2018) propose a global downscaling of subnational-level administrative data guided by the Hyde population dataset (Klein Goldewijk et al., 2011) and the global human settlement layer (Freire & Pesaresi, 2015). In addition to

GDP and GDP per capita in purchasing power parity, they also downscale the human development index in a 5-arc-min resolution (9.3 × 9.3 km grid cells at the equator) for the period 1990–2015, with temporal interpolation and extrapolation methods. The authors report the variability of the accuracy of the dataset as a drawback and a lack of uncertainty estimates.

Fang and Jawitz (2018) work at a higher resolution of 1 km, applying a power-law scaling to estimate past urban areas. They tested five different models to distribute the US population from census data, from 1790 to 2010, with the most complex model including the urban–rural divide, inhabitable land, topographic suitability and socio-economic desirability. This approach is particularly sensitive to the availability of census data. Murakami and Yamagata (2019) downscale the GDP and population scenarios developed by the SSP pathways to a 0.5° grid (approximately 50 km near the equator). They apply a four-step approach based on Global Rural–Urban Mapping (GRUMP) (Balk et al., 2006) to project a city's population value. In a first step, the approach estimates the population growth of a sample of the GRUMP cities' population with a two-stage least square (2SLS) spatial econometric model. They then define urban and rural potentials per grid based on the grid distance from the collection of cities and the project's urban and rural areas. Finally, they apply a dasymetric mapping approach to downscale rural and urban population and GDP through a multi-learning approach. Therefore, the latter considers spatial and socio-economic interactions that take into account road networks and land cover, making possible a better differentiation for urban and non-urban areas, as well as urban expansion/shrinkage. The authors suggest that using finer scale auxiliary variables and a downscaling grid of higher resolution would improve this approach. Wang and Sun (2020) compare the GDP downscaling performances of different weights based on population, nightlight and a combination of the latter two. Nightlight provides an edge for medium-sized resolutions; however, at finer scales, lost light for rural areas might introduce distortions.

Some studies propose a downscaling tailored to regional or subnational specific contexts. For instance, Merkens et al. (2016) and Reimann et al. (2018) use a methodology to downscale and assess SSP scenarios for coastal areas (the former on a global scale, and the latter for the Mediterranean area). A design flaw in these studies is their substantial difficulty in finding accurate data to categorize important factors (e.g., migration propensity to coastal areas).

Capitalizing on the insights from the previous literature, in relation to the objective of downscaling the regional ICES model's GDP projections, leads to the following considerations. First, the proposed model should work at the highest possible spatial resolution in order for the downscaling exercise to be useful for local decision-makers. Second, the use of an artificial area is recommended as a more accurate weight for the downscaling of GDP, since, in comparison with population alone, it provides a more accurate spatial distribution of economic activities. Finally, the weight should be considered endogenous and projected in the future to allow the spatial distribution of GDP to vary.

In addition, the review of the literature highlighted a tendency towards models of increasing complexity that include, for instance, gravity models with coefficients obtained from spatial econometric approaches (Kelejian & Prucha, 2002). The use of spatial econometric methods is fully justified, given the presence of spatial autocorrelation in the analysed variables. However, these are computationally demanding for sufficiently high resolutions (Arbia et al., 2019; Yamagata & Seya, 2019). Thus, this study considers the compromise solution of providing a parametrized model for the projections of the weight variable by using a multilevel modelling approach. The latter has attracted increasing interest in the social sciences, given the nested hierarchy of observed outcomes, and has been paired with spatial models, especially in health research (Corrado & Fingleton, 2011). Unfortunately, multilevel modelling does not account explicitly for a spatial form (Dong et al., 2015), but the nested structure is expected to capture some of the dependence through the random effects at different geographical scales. It must be noted that some studies have attempted to link spatial econometric insights to the multilevel approach

(Dong & Harris, 2015), but since the procedure requires the creation of a weighting matrix, the computational issue would still be present.

Another aspect worth considering is how the determinants of agglomeration processes would influence the evolution of projected economic variables. A wide literature in urban economics and old and new economic geography has studied these topics, in particular how agglomeration and dispersion forces and regional specialization impact urban spatial expansion (Fujita & Thisse, 1996). Factors such as social interactions, increasing returns, transportation costs and urban wage premiums would all contribute to agglomeration changes (Thisse, 2018). This leads to two operative considerations: the first concerns the stability of agglomeration forces over time, and the second the extent to which some determinants of agglomerations can be included in the projection procedure.

The first is addressed by considering the spatial property of path dependence. The profound technological change affecting agglomeration forces in the last century did not change the importance of historical cities (Bleakley & Lin, 2012; Rosenthal & Strange, 2020), evidencing robust spatial equilibrium patterns. This could at least sustain the idea of employing current artificial areas as the starting set for the projections.

The second is a more complex issue, as agglomeration determinants work at different geographical scales, and decay with distance (Rosenthal & Strange, 2020). As the latter work suggests, some economic variables could act as a reasonable proxy, such as commercial and industrial rent and land prices. These data are, however, not easily available and are difficult to project. The work of Viguié et al. (2014) is an example of a downscaling attempt grounded on urban economics. In that study, the authors downscale four socio-economic scenarios at the city scale for Paris, with a dynamic extension of urban economics theory. To calibrate their simulation, the authors employ figures on time and money spent on transport, real estate prices, walking time distances, actual transport times and prices of public transport. This means that the detail and granularity of these required data might be feasible for smaller contexts such as single cities, but less so for more extended maps.

Some of the variables of this study can still be considered as relevant proxies: road density, distances from the closest functional urban area (FUA), and distances from the closest airport are linked with ease of transportation and spillovers and increasing returns, while the population is an important determinant in the urban structure of the economy. One last point remains as to whether the downscaling procedure might miss some of the agglomeration 'snowball effect' which should lead in time to a more than proportional GDP share assigned to 'central' grids located in 'core' locations. Working on a detailed map of employment and productivity, Rosenthal and Strange (2020) show that manufacturing, productive activities and even R&D are quite dispersed around agglomeration hotspots, while financial services are most concentrated in downtown urban areas. The downscaling of this work, using artificial areas as the main weight, could then lose the concentration effect of financial services. However, it must be noted that the climate impacts modelled in ICES are regarded more as a direct effect on selected sectors rather than the indirect financial ones, while the latter are very important in the context of climate change (Campiglio et al., 2018), local adaption policies would need a data reference that considers the spatial dispersion of the affected sectors.

## 3. METHODOLOGY

Following the insights from the literature, in particular the studies based on urban potentials (Jones & O'Neill, 2016; Murakami & Yamagata, 2019), the present study downscales GDP according to two of its main determinants: urban (or artificial) area and the population at the grid level, conditioned by the contribution of available spatial auxiliary variables.

This approach departs methodologically from urban gravity potential methods. While the projection of urban potentials is usually based on a sample of the greatest urban population, here the analysis is kept at the grid level. The main reason is that the starting grid dataset is already endowed with population figures downscaled for 2006 and 2011. The growth of each urban (or artificial) area grid is conditioned directly by the evolution of the grid's total population, used as weight. This information also allows for discounting the contribution of inhabited rural areas to the distribution of GDP levels to each grid. Another deviation is that instead of selecting a final model through averaging the contribution to urban areas by the different auxiliary variables (e.g., through ensemble learning, as in Murakami & Yamagata, 2019), all the variables are directly included in an econometrically parametrized model. The resulting projections of urban areas are conditioned by the auxiliary variables of each grid's fixed cell effects.

This procedure results then in a straightforward three-step ~~grid-level~~ model. First, population counts $P$ per grid $g$ are projected through a share of growth method using country-level SSP population growth rates scenarios. Second, urban and artificial area ($UA$) per grid is projected by using projected population values and coefficients obtained from a linear mixed model that includes auxiliary variables. Third, the GDP regional values from ICES are downscaled at the grid level by using the projected urban area values as weights.

### 3.1. First step: Population projections

Grid-level urban area projections are conditioned by one primary time-varying variable: population per grid. The starting point of the procedure is the 2011 value of gridded population, used to create the projected grid population associated with a country-level scenario by using the share of growth method (Yamagata et al., 2015). This method links the population ($P$) growth of a lower scale unit (the grid $g$) to that at an upper (and available) level (the country $C$) at times $T$, $t$ and $t-\tau$:

$$P_{T,g} = P_{t,g} + (P_{T,C} - P_{t,C}) \frac{(P_{t,g} - P_{t-\tau,g})}{(P_{t,C} - P_{t-\tau,C})} \tag{1}$$

The method is applied by considering the countries' total population growth rates available from the SSP scenarios (Riahi et al., 2017).[2] Four main urban area trajectories are defined, based on the different population projections at the country level, which correspond to SSP1 'Sustainability (Taking the Green Road)', SSP2 'Middle of the Road', SSP3 'Regional Rivalry (A Rocky Road)' and SSP5 'Fossil-fueled Development (Taking the Highway)'.

### 3.2. Second step: Urban area projections

The second step is to model urban area per grid $g$ in the starting year $t$, $\mathrm{UA}_g^t$ based on population P and a matrix of $k$ auxiliary variables $X_g$. To account for the hierarchically nested structure of the grids in the administrative units – each grid is part of groupings of increasing size, namely local urban area (LAU) $l$, NUTS-3 province $n$, NUTS-2 region $r$ and country $c$ – we employ a linear mixed model (West et al., 2014) that characterizes the response variable with a standard fixed term and hierarchically clustered random effects:

$$\log(UA_{g,l,n,r,c}) = \alpha + \beta_1 \log(P_{g,l,n,r,c}) + \beta_k X^k_{g,l,n,r,c} + \lambda_l + \eta_n + \rho_r + \zeta_c + \varepsilon_{g,l,n,r,c} \tag{2}$$

In equation (2), the most general formulation, that is, the urbanized area in grid $g$, which is part of city $l$, province $n$, region $r$ and country $c$ ($UA_{g,l,n,r,c}$), depends on population per grid cell ($P_{g,l,n,r,c}$), and a set of $k$ auxiliary variables $X^k_{g,l,n,r,c}$, including the log of the distance from the nearest coast, the log of the distance from the nearest border, the log of the distance from the closest FUA centroid, the grid's road density, the grid's land percentage rescaled to 0–1, and the ratio between 2011 grid population level and its 2006 value. The composite error term is made by

the different administrative cluster-specific random effects ($\lambda_l$, $\eta_n$, $\rho_r$, $\zeta_c$), in addition to the standard i.i.d. error term $\varepsilon$.[3]

As already discussed, the advantage of this modelling choice lies in its computational feasibility. While different approaches based on urban potentials and spatial econometrics could be better suited in the presence of spatial autocorrelation in the data, the computational burden would only allow us to obtain a final downscaling of a much-reduced resolution (Yamagata & Seya, 2019). As an example, notwithstanding the differences of the countries included or not in ICES, the grid map with a 20 × 20 km resolution for Europe has 19,694 observations, which would require substantial computational power for the generation of a distance matrix and could be treated only with the most forgiving methods, such as spatial 2SLS. The administrative units below the NUTS-3 classification are the local administrative area (LAU), which for the 2019 version declares 102,482 units, an even less tractable number.

By considering the population coefficient value from the best model, each grid $g$ urban area value is projected to a target year $T$. Equation (3) presents this process:

$$log(\widehat{UA}_g^T) = log(\widehat{UA}_g^t) + \hat{\beta}_1(log(\tilde{P}_g^T) - log(\tilde{P}_g^t)) \tag{3}$$

The difference between the projected population values per grid in years $T$ and $t$ increases or decreases the projected values of urban area in year $T$. We iterate this procedure in five-year intervals from 2015 to the ICES end year, 2070.

It must be highlighted that this method operates on the simplifying assumption that the time-invariant exogenous variables will cancel out their effects over time. While this assumption is, overall, unrealistic for at least some of the variables employed as fixed effects, it needs to be considered, given the unavailability of the 2050 projections' values.

Moreover, to avoid unrealistic results, the projections are bound to a set of assumptions. The first is that the projected urban area cannot be higher than the land percentage of the grid, which provides a maximum value of the buildable area. The assumption implies that expanding the urban area would overcome any rural or natural area but would not grow on water surfaces. The second assumption is that urbanization is assumed to be irreversible, meaning that if the prediction by the model sets a decrease in the urban area, the level is fixed as the $T - 5$ one. This fits the data-based urban area definition (see section 4), as actually a collection of artificial areas that could fit different purposes (such as activities and services), aside from population dwellings. The last assumption is that the method conditions the urban area's minimum value to the last year of the actual available data, 2018.

### 3.3. Third step: GDP downscaling projections

Finally, the GDP projections from ICES are downscaled by aggregating the ICES model's regions $R$ projected urban area for a given year, and distributing the GDP levels according to the grid share of urban area over the whole region, as shown in equation (4):

$$GDP_g^t = \frac{\widehat{UA}_g^t}{\widehat{UA}_R^t} GDP_R^t \tag{4}$$

where $GDP_R^t$ is the GDP level in region $R$ and year $t$ generated for each given scenario combinations of the ICES model; $\widehat{UA}_g^t$ are the values of the urban area projected in the previous step; and $\widehat{UA}_R^t$ is the aggregation at the regional level of those values.

The next section describes in detail the data used to calibrate the procedure.

## 4. DATA

The ICES model provides GDP levels in NUTS regions for selected scenarios and climate impacts. The scenarios combine SSPs and representative concentration pathways (RCPs) (van Vuuren et al., 2011). Moreover, the model takes population projections as an exogenous variable and provides endogenous GDP and emissions levels according to a calibration that follows the different SSP-RCP combinations. The downscaling procedure takes these GDP projections as their primary exogenous input (see Table A1.1 in Appendix A in the supplemental data online for the regions included).

First, to perform the downscaling, we selected the grid system for the geographical reference that is consistent with previous environmental research (Nam & Reilly, 2013), the 1 × 1 km grid map of Europe from GISCO[4] being the highest one at the time of writing.

Urban area is obtained from remote satellite sensing of Copernicus CORINE Land Cover (CLC). For each grid, area is summed over the CLC codes '1 – Artificial Surfaces', which include urban fabric, industrial, commercial, and transport units, mine dump and construction sites, and other artificial non-agricultural areas.

Population values per grid are already present in the GISCO grid map for 2006 and 2011. Values for subsequent years are obtained through a share of growth method, which requires three points in time to iterate the formula, whether or not the initial dataset used has only two. Therefore, we obtain the first downscaling at the grid level for 2015 with a more straightforward method known as a 'constant share of growth' (Yamagata et al., 2015), where the growth rate is equally shared across a region's grids. The 2015 value is computed as the third point, and the actual population levels from Eurostat data are derived for 2015 and 2011. The grid's population is projected by using the growth rates for the population in the selected SSP values from the International Institute for Applied Systems Analysis (IIASA) model (Riahi et al., 2017).

The other variables employed are already part of the GISCO grid dataset. Land percentage presents the share of land per grid compared with water and other non-classified areas. Border distance[5] is the distance from the closest national border. Coast distance is the distance from the closest sea or ocean grid. Population values for 2011 and 2006 are combined to compute population growth from 2006.

Additional variables included are the distances (km) of the grid from the nearest airport (D. airport), seaport (D. port), and the closest FUA as per the 2018 definition (D. FUA); the road density in metres of roads per $km^2$ retrieved from the Global Roads Inventory Project (GRIP) dataset (Meijer et al., 2018). Table 1 presents the variables used with their sources. The summary statistics are presented in Table A1.2 in Appendix A in the supplemental data online.

## 5. RESULTS

### 5.1. Results

The first intermediate step was to project the population count at the grid level for the different SSP scenarios. Table A1.3 in Appendix A in the supplemental data online reports the descriptive statistics for the projected population counts in 2050. SSP5 shows the highest mean value per grid, while SSP3 has the lowest.

The second step in the procedure was to project urban area at the grid level, following the model proposed in equation (2). First, we verified that the model with fixed effects improves the marginal and conditional $R^2$, compared with a random-intercept and population only. Second, keeping the fixed part of the model stable, we compared multiple possible specifications of their random effects. Table 2 presents these different versions, indexed from (1) to (5) according to their random effects specifications: model (1) includes only NUTS-3 level random effects,

**Table 1.** Description and source of the variables.

| Variable | Description | Source |
|---|---|---|
| UA | Area ($m^2$) per grid | CORINE Land Cover, Copernicus Land Monitoring Service |
| Grid | Grid for the European area at a 1 km resolution | GEOSTAT1 and GEOSTAT 2006 initiative of the European Commission |
| Population per grid (2006, 2011, 2018), *P.* ratio | Population values by grid | |
| Land percentage | Share of land per grid | |
| Country ID and NUTS classification (0, 1, 2, 3 levels) | Code for the administrative location of the grid, in NUTS 2016 classification | |
| D. Border | Distance (km) from the closest national border | |
| D. Coast | Distance (km) from the closest ocean or sea | |
| D. Airport | Distance (km) from the grid's closest airport | Point dataset 'airports 2013', European Commission GISCO, 'Transport networks' |
| D. FUA | Distance (km) from the closest functional urban area (as per the 2018 definition) | European Commission GISCO, 'Urban Audit' |
| Road density | Metres of roads per $m^2$ | Global Roads Inventory Project, GLOBIO (Meijer et al., 2018) |
| GDP projections | Projections by the ICES model at the regional level for the selected scenarios | ICES |
| Population SSP trends | Country-level total population growth rates for the selected SSP scenarios | IIASA (Riahi et al., 2017) |

model (2) includes NUTS-3 and NUTS-2 nested random effects, model (3) presents NUTS-2 and country nested random effects, model (4) includes NUTS-3, NUTS-2 and country random effects, and model (5) includes nested LAU, NUTS-3 and NUTS-2 random effects. The change in the random effects specification does not seem to substantially affect the coefficients' slope and magnitude.

As largely expected, the population coefficient is positive and statistically significant. Road density and land percentage also display positive impacts. Distance variables are negatively sloped, consistent with the urban gradient hypothesis, their largest effect being noticeable in the case of airports. Population growth in the 2006–11 period also has a negative sign, which offers no particularly straightforward interpretation, because the growth from 2006 to 2011 is positive and should be intuitively linked to an increase in urban area. However, it must be noted that a high positive ratio in fully occupied grids or in grids with low values of urban area might confound this effect in a cross-section setting.

According to the analysis of variance (ANOVA) results, the model with regional (both lower and higher levels, NUTS-3 and -2, respectively) and country random effects (NUTS-4) should be preferred to the other specifications. This model was then used to project urbanized areas and

**Table 2.** Estimation results of the models with all fixed effects.

| | (1) | (2) | (3) | (4) | (5) |
|---|---|---|---|---|---|
| log *P* | 0.041*** | 0.041*** | 0.041*** | 0.041*** | 0.041*** |
| | (0.000) | (0.000) | (0.000) | (0.000) | (0.000) |
| log d. coast | −0.002*** | −0.002*** | −0.001*** | −0.002*** | −0.007*** |
| | (0.000) | (0.000) | (0.000) | (0.000) | (0.000) |
| log d. border | −0.003*** | −0.003*** | −0.003*** | −0.003*** | −0.003*** |
| | (0.000) | (0.000) | (0.000) | (0.000) | (0.000) |
| log d. FUA | −0.002*** | −0.002*** | −0.001*** | −0.002*** | −0.012*** |
| | (0.000) | (0.000) | (0.000) | (0.000) | (0.000) |
| log d. airport | −0.007*** | −0.007*** | −0.006*** | −0.007*** | −0.014*** |
| | (0.000) | (0.000) | (0.000) | (0.000) | (0.000) |
| log *P.* ratio | −0.066*** | −0.066*** | −0.068*** | −0.066*** | −0.061*** |
| | (0.000) | (0.000) | (0.000) | (0.000) | (0.000) |
| log road density | 0.000*** | 0.000*** | 0.000*** | 0.000*** | 0.001*** |
| | (0.000) | (0.000) | (0.000) | (0.000) | (0.000) |
| land percentage | 0.004*** | 0.004*** | 0.005*** | 0.005*** | 0.005*** |
| | (0.000) | (0.000) | (0.000) | (0.000) | (0.000) |
| Constant | 0.116*** | 0.121*** | 0.091*** | 0.123*** | 0.399*** |
| | (0.002) | (0.002) | (0.004) | (0.004) | (0.003) |
| Observations | 4,436,642 | 4,436,642 | 4,436,642 | 4,436,642 | 4,339,077 |
| Log-likelihood | 5,073,093 | 5,073,741 | 5,016,659 | 5,074,010 | 5,028,587 |
| Akaike information criterion (AIC) | −10,146,164 | −10,147,459 | −10,033,294 | −10,147,992 | −10,057,147 |
| Bayesian information criterion (BIC) | −10,146,018 | −10,147,299 | −10,033,134 | −10,147,806 | 10,056,975 |

(*Continued*)

**Table 2.** Continued.

| | (1) | (2) | (3) | (4) | (5) |
|---|---|---|---|---|---|
| Marginal $R^2$ | 0.493 | 0.493 | 0.525 | 0.495 | 0.362 |
| Conditional $R^2$ | 0.640 | 0.640 | 0.608 | 0.640 | 0.725 |

Note: Model (1) includes NUTS-3 random effects; model (2) includes nested NUTS-3 and NUTS-2 random effects; model (3) includes nested NUTS-2 and country random effects; model (4) includes nested NUTS-3, NUTS-2 and country random effects; and model (5) includes nested NUTS-2, NUTS-3 and LAU random effects. Standard errors are shown in parentheses.
***Significant at the 1% level;
**significant at the 5% level;
*significant at the 10% level.

distribute the regional projected GDP. Urban area projections are summarized in Table A1.3 in Appendix A in the supplemental data online. There are differences in the means, standard deviations and, noteworthy, in the third quartile of the distribution. By comparing these summary measurements across scenarios, Table A1.3 online provides an overview of how the different SSPs would lead to a change in the spatial distribution of an urban area and, ultimately, its economic activity. The differences between these values and those from 2018 for the scenario SSP2 are mapped in Figure A2.1 online.

The downscaled GDP data cover the SSP-RCP scenario combinations generated by ICES, and are divided into baseline version and low, medium and high levels of climate impacts. This projected dataset was further divided into high and low mobility of investments,[6] for a final figure set of 72 different geo-referenced projected GDP time series (a description of the data specifics is provided in Appendix A3 in Appendix A in the supplemental data online).

Figures 1 and 2 present some selected maps generated from the results dataset from the high mobility of investments version. Figure 1 shows a magnified zoom over Europe depicting 2015, the first year of the downscaled GDP levels taken from the ICES scenario in the SSP1-RCP2.6 combination. Figure 2 maps the absolute change of GDP levels in 2050 keeping a high climate impact fixed, and the high mobility of investment, comparing the scenario SSP2-RCP2.6 against the SSP2-RCP4.5 (Figure 2a) and the SSP2-RCP6.0 (Figure 2b). Summary statistics about the downscaled GDP series are reported in Tables A1.4 and A1.5 in Appendix A in the supplemental data online.

## 5.2. Validation

In this subsection, we perform some validation and robustness checks. First, we compare our results with those applying similar procedures proposed in the literature and show the relative

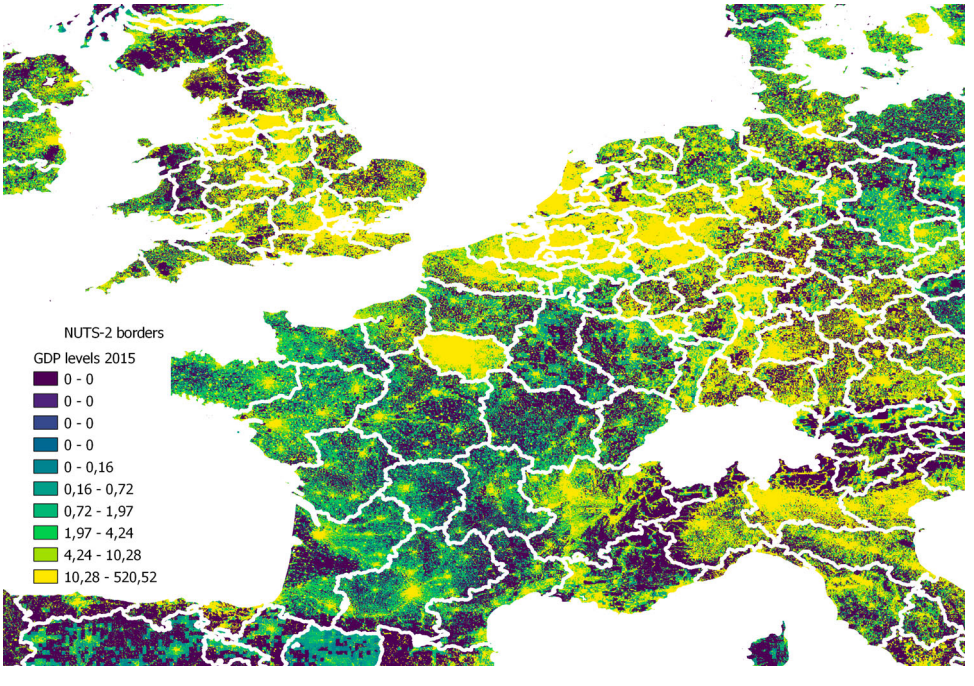


**Figure 1.** Magnified gross domestic product (GDP) levels in 2015 in 2007 million US$, scenario SSP1-RCP2.6 (high mobility of investments version).

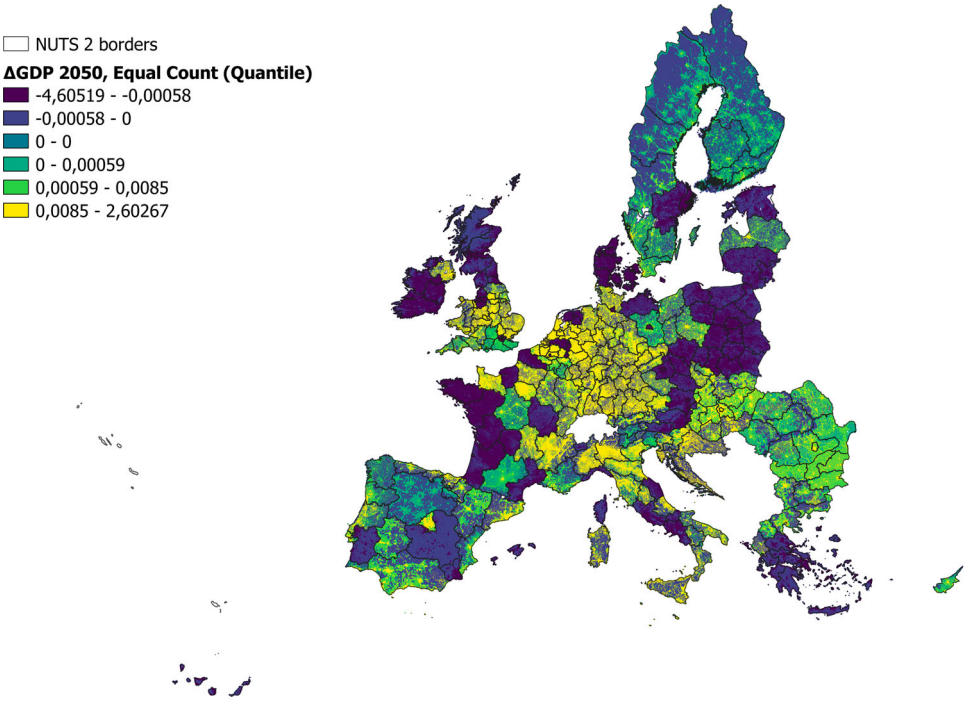


(a)

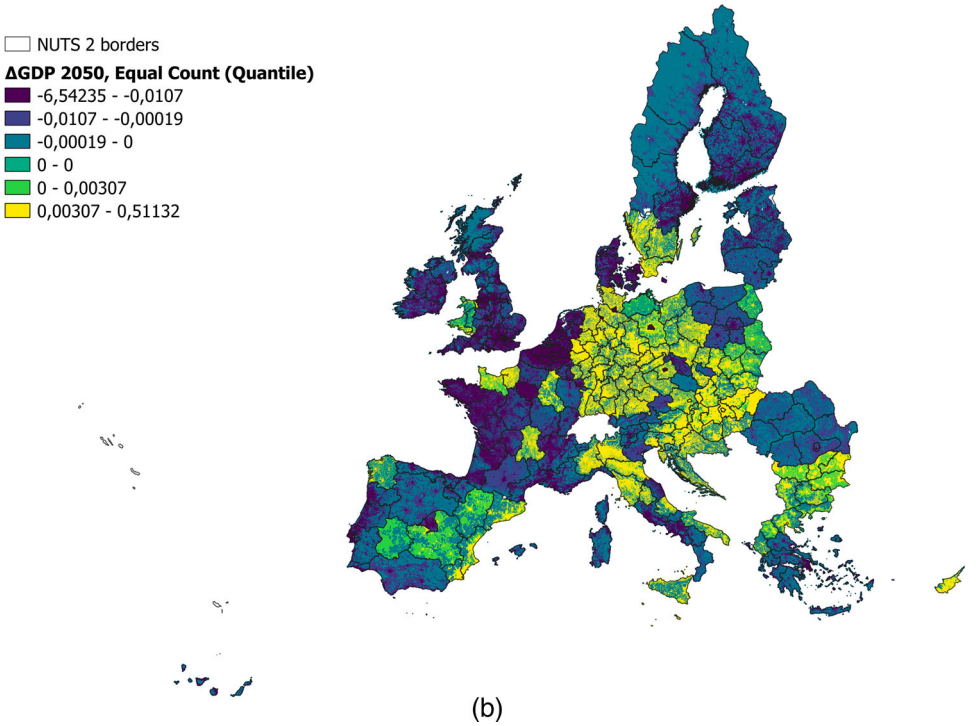


(b)

**Figure 2.** Absolute difference of the downscaled projected gross domestic product (GDP) in 2050 for scenario SSP2 with a high climate impact (high mobility of investments version) between different RCP scenarios: (a) SSP2-RCP2.6 – SSP2-RCP4.5; and (b) SSP2-RCP2.6 – SSP2-RCP6.0.

accuracy of our approach. Second, we consider a spatial econometric specification for the urbanized area model and demonstrate that mixed models, which are much more feasible for large data samples, produce results that match those obtained by taking space explicitly into account, as in spatial econometric models. Finally, we validate our results, using sample estimates to make out-of-sample predictions, both leaving one time out and one group out.

### 5.2.1. *Comparison with similar work*

To compare our downscaling approach with existing ones, we looked at the produced GDP series. To make the comparison easier and more interpretable, we aggregate grid-level data at the urban level, considering the FUA as reference spatial unit. First, we took the reference year 2015 and compare our FUA-level GDP with that produced by Kummu et al. (2020), which is available for the same year. Second, we make another comparison with the values produced by Murakami and Yamagata (2019), this time for the reference year 2050.

GDP levels in millions at the FUA level are available in 2015 at constant prices from the Organisation for Economic Co-operation and Development (OECD) (2012). Selecting only the metropolitan areas included in the ICES model regions resulted in a set of 301 observations across 27 countries. The downscaled GDP values for scenario SSP2-RCP4.5 for 2015 were then aggregated by using each metropolitan area perimeter as a mask. The same procedure was applied to the 30 arc-sec (approximately 1 km) downscaled GDP values for 2015 obtained from Kummu et al. (2020); all monetary values are then converted into the same monetary unit. In Figure 3 the first panel presents a comparison of the data between the FUA GDP and the re-aggregated ones from this work and shows that our approach assigns higher GDP values to cities with higher incomes. The second panel presents a mirror bar chart that shows the delta in the absolute value of GDP between the present study and Kummu et al. (2020). Overall, the latter displays a lower normalized RMSE with respect to the current work (0.243 versus 0.278). Since it applies a direct downscaling based on gridded population weights, the loss of precision due to the modelling part of the current approach appears to be within a comparable order of magnitudes, even outperforming it even in some metropolitan areas.

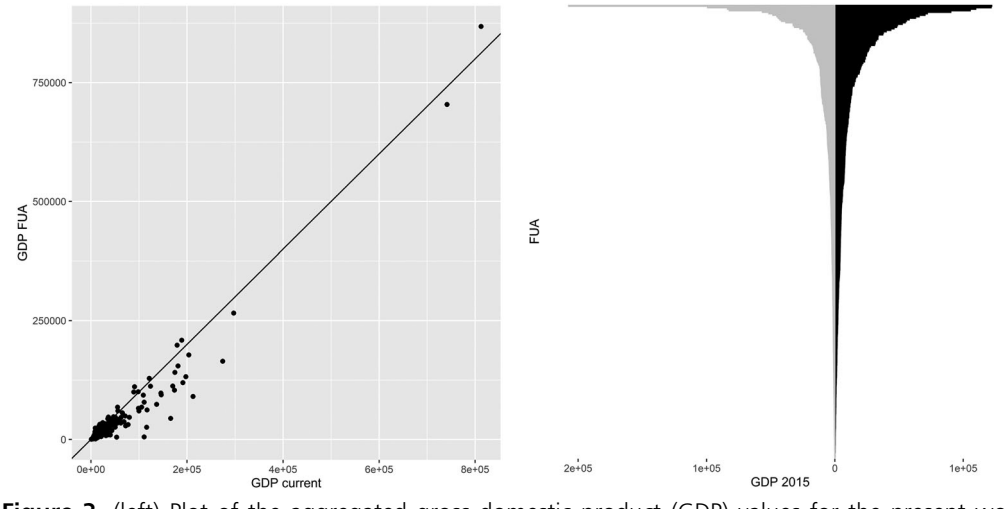


**Figure 3.** (left) Plot of the aggregated gross domestic product (GDP) values for the present work against Organisation for Economic Co-operation and Development (OECD) data for 2015 at the functional urban area (FUA) level; and (right) mirror bar chart of the differences between the OECD's FUA data and the FUA aggregated GDP values from Kummu et al. (2020) (grey) and the present work (black).

Since the focus of this work is on future projections, an additional comparison is provided for 2050. This was not a straightforward task, as working with future values entails a lack of actual data for the evaluation. Thus, another projected series was recovered from an available dataset (Murakami & Yamagata, 2019) that includes downscaled data consistent with the SSP scenario projections. In contrast to it, we used a combination of SSP and the RCP scenarios for GDP projections, and so aggregated GDP figures differ and are not perfectly comparable. The baseline of the SSP2-RCP45 scenario appears to be the one with higher comparability and was used for this validation exercise. In addition, it is worth noting that Murakami and Yamagata (2019) used a lower resolution (approximately 50 km). Thus, we aggregated our values by using their grid layer to have comparable figures. Figure 4 plots the two GDP series against each other. The most significant differences are observed in the grids with a higher GDP value.

### 5.2.2. *Spatial autocorrelation*

Given the plausible presence of spatial autocorrelation, a test was performed on some subsets of the data that serves to ascertain whether addressing the issue with a more explicit methodology

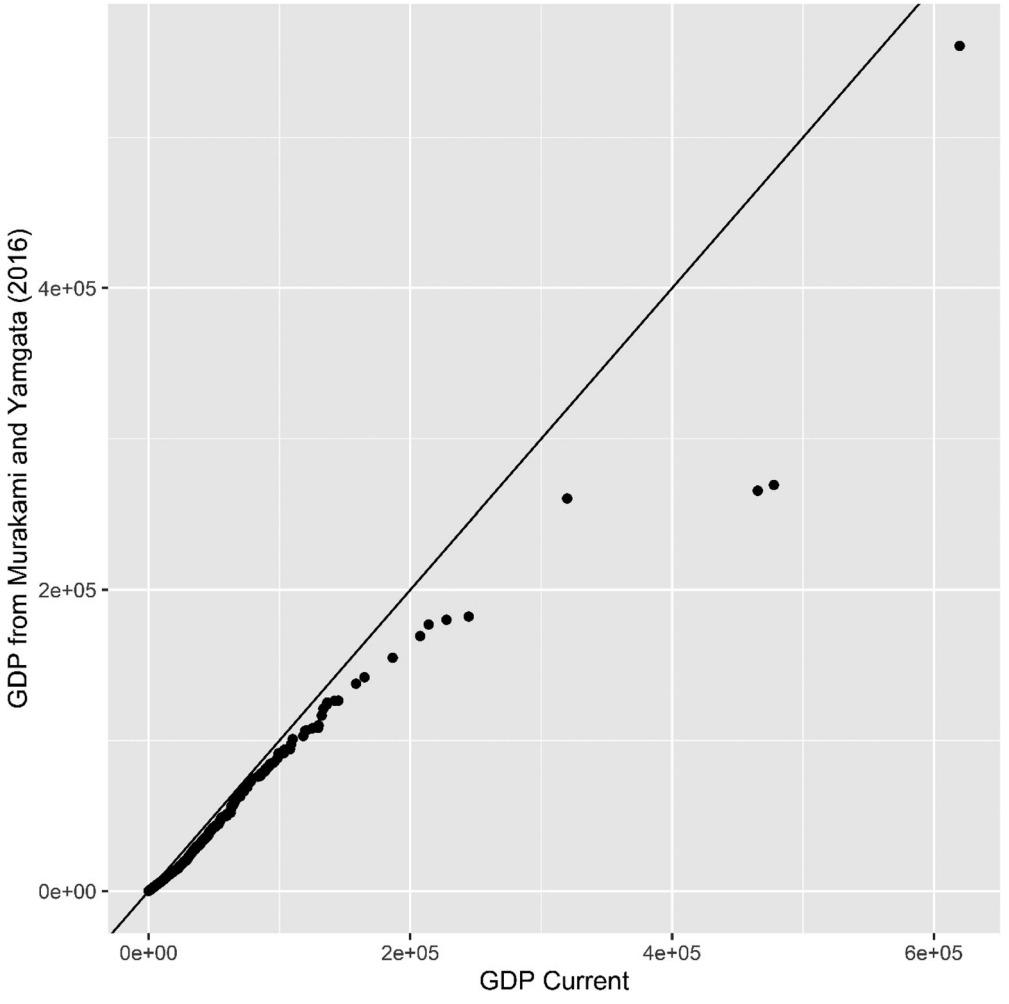


**Figure 4.** Murakami and Yamagata's (2019) downscaled gross domestic product (GDP) for 2050 SSP2 versus the current work downscaled GDP for SSP2-RCP45.

would significantly change the estimated population parameter. The subsets were restricted to a much lower number of observations to allow the computational feasibility of the procedure. The subsample models were regressed with the '*nmle*' package (Pinheiro et al., 2022), which makes possible hierarchical linear mixed models with different spatial autocorrelation structures. Using Gaussian and spherical spatial autocorrelation structures for some NUTS-2 units (ITH4, ITF2) and some small country (MT) ones returns positive and significant coefficients for population fixed effects, with values ranging from 0.004 to 0.001, in line with those obtained in the previous section.

### 5.2.3. *Projecting 2018 urban area*

The urban area for 2018 was projected at the grid level and compared with the actual 2018 data. The latter is available and was collected using the same method as for 2012. The urban area downscaling procedure is applied equivalently to section 3, but employs the downscaled population values for 2020. Table A1.6 in Appendix A in the supplemental data online shows summary statistics for the actual 2018 values and the projected urban areas (one for each population SSP). Projected values show a greater mean and similar standard deviation. Explanatory factors for this feature could include not considering external regulatory limitations to urban area expansion and potential mismatches between the satellite imagery's area classification procedure and the population counts per grid. Differences between projections, which are led by the changes in population, are minimal. This follows the fact that in the year of this test populations have not diverged much.

### 5.2.4. K-*fold cross-validation*

A *K*-fold cross-validation procedure was run for the model of equation (2). The model was tested after subtracting observations belonging to the highest categorization group, namely countries, from the dataset. The subtracted country values were then predicted with the ~~test~~ dataset results. The procedure was iterated for each country, and the differences between the actual and the predicted values were used to calculate the RMSE. The only model that failed to converge is the one without observations from France. The final predictions resulted in an RMSE of 0.082.

## 6. CONCLUSIONS

To better assess the local economic costs of global climate change and the economic benefits of acting early for adaptation in the different scenarios, we propose a methodology that can consistently downscale integrated model output from the regional to the grid level. The advantage of this methodology is its tractability, which comes in tandem with the capacity to accurately represent the spatial distribution of economic activity through the observed and projected urbanized area. Multilevel models with hierarchically organized random effects make the projection of urbanized area feasible even in extensive spatial data samples. We validated this approach by demonstrating its out-of-sample performance when predicting future values and values in a region not considered in the sample. In addition, we have shown that the multilevel approach provides, at least in the context of this work, comparable results with spatial econometric models.

As a caveat, additional refinements to the parametrized model should be tested, as well as some robustness checks and validation procedures. For instance, it would be interesting to resume the analysis with a generalized linear method and with other distributions that could better fit the data, although, given the fine spatial resolution of 1 km, the computational burden would be substantial. Moreover, more involved random effects and additional time-varying variables could help to obtain more precise results.

Besides the visualization of the climate impacts, this exercise could act as a solid basis for developing more complex methods that can be useful to represent a significant spatial change

in GDP distribution due to climate impacts. A promising example regards the differentiation of climate shocks. If a shock could be categorized appropriately with respect to its impact on a specific variable that can be included in this method, then the spatial distribution should also change within the given region in the same scenario.

To conclude, downscaling the projections of GDP changes due to different scenarios and climate impacts is a relevant exercise, as it lays the basis for a properly spatial understanding of what is to come at resolutions far lower than those usually employed by climate change economic assessments. This information is very important to the policymaker, who could therefore apply its finite resources in a far more precise and efficient effort to prevent and contrast climate change impacts.

## ACKNOWLEDGEMENTS

We gratefully acknowledge the comments and suggestions from the participants in the ninth Italian Association of Environmental and Resource Economists (IAERE) Annual Conference (online, April 21-23, 2021) and from the two anonymous referees. Errors remain our own.

## DISCLOSURE STATEMENT

No potential conflict of interest was reported by the authors.

## NOTES

[1] Nomenclature of Territorial Units for Statistics; see https://ec.europa.eu/eurostat/web/nuts/background/.
[2] The same scenarios are used in the ICES model to produce GDP projections.
[3] The model is fitted with restricted maximum likelihood with the *lme4* package of software *R* (Bates et al., 2015).
[4] Geographical Information System of the European Commission.
[5] Every distance is intended as that from the centroid of the referenced grid.
[6] The high and low mobilities of investments refer to different assumptions made within the ICES to model the level of capital market integration. These assumptions can play a role in the macro-economic assessment of climate change for specific impacts such as sea level rise or riverine floods, but do not change the baseline scenarios in terms of GDP and population trends.

## ORCID

*Massimiliano Rizzati* http://orcid.org/0000-0003-0574-8934
*Gabriele Standardi* http://orcid.org/0000-0002-4989-2201
*Gianni Guastella* http://orcid.org/0000-0002-1333-4718
*Ramiro Parrado* http://orcid.org/0000-0002-0951-1013
*Francesco Bosello* http://orcid.org/0000-0001-8492-219X
*Stefano Pareglio* http://orcid.org/0000-0001-6274-7511

## REFERENCES

Arbia, G., Ghiringhelli, C., & Mira, A. (2019). Estimation of spatial econometric linear models with large datasets: How big can spatial Big data be? *Regional Science and Urban Economics*, *76*, 67–73. https://doi.org/10.1016/j.regsciurbeco.2019.01.006

Asadoorian, M. O. (2008). Simulating the spatial distribution of population and emissions to 2100. *Environmental and Resource Economics*, *39*(3), 199–221. https://doi.org/10.1007/s10640-007-9105-8

Balk, D. L., Deichmann, U., Yetman, G., Pozzi, F., Hay, S. I., & Nelson, A. (2006). Determining global population distribution: Methods, applications and data. *Advances in Parasitology*, *62*, 119–156. https://doi.org/10.1016/S0065-308X(05)62004-0

Bates, D., Maechler, M., Bolker, B., & Walker, S. (2015). Fitting Linear Mixed-Effects Models Using lme4. *Journal of Statistical Software*, *67*(1), 1–48. https://doi.org/10.18637/jss.v067.i01

Bengtsson, M., Shen, Y., & Oki, T. (2006). A SRES-based gridded global population dataset for 1990–2100. *Population and Environment*, *28*(2), 113–131. https://doi.org/10.1007/s11111-007-0035-8

Bleakley, H., & Lin, J. (2012). Portage and path dependence. *The Quarterly Journal of Economics*, *127*(2), 587–644. https://doi.org/10.1093/qje/qjs011

Bosello, F., & Standardi, G. (2018). A Sub national CGE model for the European Mediterranean countries. In F. Perali, & P. L. Scandizzo (Eds.), *The New generation of Computable general Equilibrium models* (pp. 279–308). Springer International.

Campiglio, E., Dafermos, Y., Monnin, P., Ryan-Collins, J., Schotten, G., & Tanaka, M. (2018). Climate change challenges for central banks and financial regulators. *Nature Climate Change*, *8*(6), 462–468. https://doi.org/10.1038/s41558-018-0175-0

Carleton, T. A., & Hsiang, S. M. (2016). Social and economic impacts of climate. *Science*, *353*(6304), aad9837. https://doi.org/10.1126/science.aad9837

CIESIN. (2004). *WRI, 2000. Gridded population of the world (GPW), version 2*. Center for International Earth Science Information Network (CIESIN), Columbia University, International Food Policy Research Institute (IFPRI) and World Resources Institute (WRI).

Corrado, L., & Fingleton, B. (2011). *Multilevel modelling with spatial effects. Discussion paper*. University of Strathclyde.

DCW (Digital Chart of the World). (n.d.). Data set developed by ESRI (Environmental Systems Research Institute, Inc., USA). http://worldmap.harvard.edu/data/geonode:Digital_Chart_of_the_World.

Dobson, J. E., Bright, E. A., Coleman, P. R., Durfee, R. C., & Worley, B. A. (2000). Landscan: A global population database for estimating populations at risk. *Photogrammetric Engineering and Remote Sensing*, *66*(7), 849–857. https://doi.org/10.1201/9781482264678-24

Dong, G., & Harris, R. (2015). Spatial autoregressive models for geographically hierarchical data structures. *Geographical Analysis*, *47*(2), 173–191. https://doi.org/10.1111/gean.12049

Dong, G., Harris, R., Jones, K., & Yu, J. (2015). Multilevel modelling with spatial interaction effects with application to an emerging land market in Beijing, China. *PloS one*, *10*(6), e0130761. https://doi.org/10.1371/journal.pone.0130761

Elvidge, C. D., Baugh, K. E., Kihn, E. A., Kroehl, H. W., & Davis, E. R. (1997). Mapping of city lights using DMSP operational linescan system data. *Photogrammetric Engineering and Remote Sensing*, *63*(6), 727–734.

Fang, Y., & Jawitz, J. W. (2018). High-resolution reconstruction of the United States human population distribution, 1790 to 2010. *Scientific Data*, *5*(1), 180067. https://doi.org/10.1038/sdata.2018.67

Farmer, J. D., Hepburn, C., Mealy, P., & Teytelboym, A. (2015). A third wave in the economics of climate change. *Environmental and Resource Economics*, *62*(2), 329–357. https://doi.org/10.1007/s10640-015-9965-2

Forslid, R., & Ottaviano, G. I. (2003). An analytically solvable core-periphery model. *Journal of Economic Geography*, *3*(3), 229–240. https://doi.org/10.1093/jeg/3.3.229

Freire, S., & Pesaresi, M. (2015). GHS population grid, derived from GPW4, multitemporal (1975, 1990, 2000, 2015). European Commission, Joint Research Centre (JRC)[Dataset] PID: http://data.europa.eu/89h/jrc-ghsl-ghs_pop_gpw4_globe_r2015a.

Fujimori, S., Abe, M., Kinoshita, T., Hasegawa, T., Kawase, H., Kushida, K., Masui, T., Oka, K., Shiogama, H., Takahashi, K., Tatebe, H., & Yoshikawa, M. (2017). Downscaling global emissions and its implications derived from climate model experiments. *PloS one*, *12*(1), e0169733. https://doi.org/10.1371/journal.pone.0169733.

Fujita, M., & Thisse, J. F. (1996). Economics of agglomeration. *Journal of the Japanese and International Economies*, *10*(4), 339–378. https://doi.org/10.1006/jjie.1996.0021

Gaffin, S. R., Rosenzweig, C., Xing, X., & Yetman, G. (2004). Downscaling and geo-spatial gridding of socio-economic projections from the IPCC special report on Emissions Scenarios (SRES). *Global Environmental Change*, *14*(2), 105–123. https://doi.org/10.1016/j.gloenvcha.2004.02.004

Gambhir, A., Drouet, L., McCollum, D., Napp, T., Bernie, D., Hawkes, A., … Lowe, J. (2017). Assessing the feasibility of global long-term mitigation scenarios. *Energies*, *10*(1), en10010089. https://doi.org/10.3390/en10010089

Gao, J.. (2017). *Downscaling global spatial population projections from 1/8–degree to 1–km grid cells*. Boulder, CO: National Center for Atmospheric Research. http://dx.doi.org/10.5065/D60Z721H. .

Grübler, A., O'Neill, B., Riahi, K., Chirkov, V., Goujon, A., Kolp, P., … Slentoe, E. (2007). Regional, national, and spatially explicit scenarios of demographic and economic change based on SRES. *Technological Forecasting and Social Change*, *74*(7), 980–1029. https://doi.org/10.1016/j.techfore.2006.05.023

Jones, B., & O'Neill, B. C. (2013). Historically grounded spatial population projections for the continental United States. *Environmental Research Letters*, *8*(4), 044021. http://dx.doi.org/10.1088/1748-9326/8/4/044021

Jones, B., & O'Neill, B. C. (2016). Spatially explicit global population scenarios consistent with the Shared Socioeconomic pathways. *Environmental Research Letters*, *11*(8), 084003. http://dx.doi.org/10.1088/1748-9326/11/8/084003

Kelejian, H. H., & Prucha, I. R. (2002). 2SLS and OLS in a spatial autoregressive model with equal spatial weights. *Regional Science and Urban Economics*, *32*(6), 691–707. https://doi.org/10.1016/S0166-0462(02)00003-0

Klein Goldewijk, K., Beusen, A., Van Drecht, G., & De Vos, M. (2011). The HYDE 3.1 spatially explicit database of human-induced global land-use change over the past 12,000 years. *Global Ecology and Biogeography*, *20*(1), 73–86. https://doi.org/10.1111/j.1466-8238.2010.00587.x

Kummu, M., Taka, M., & Guillaume, J. H. (2018). Gridded global datasets for gross domestic product and Human Development Index over 1990–2015. *Scientific Data*, *5*(1), 180004. https://doi.org/10.1038/sdata.2018.4

Kummu, M., Taka, M., & Guillaume, J. H. A. (2020). Data from: Gridded global datasets for Gross Domestic Product and Human Development Index over 1990–2015, Dryad, Dataset, https://doi.org/10.5061/dryad.dk1j0.

Masson-Delmotte, V., Zhai, P., Pörtner, H. O., Roberts, D., Skea, J., Shukla, P. R., Pirani, A., Moufouma-Okia, W., Péan, C., Pidcock, R., Connors, S., Matthews, J. B. R., Chen, Y., Zhou, X., Gomis, M. I., Lonnoy, E., Maycock, T., Tignor, M., & Waterfield, T.. (2018). IPCC, 2018: Summary for Policymakers. In *Global Warming of 1.5°C. An IPCC Special Report on the impacts of global warming of 1.5°C above pre-industrial levels and related global greenhouse gas emission pathways, in the context of strengthening the global response to the threat of climate change, sustainable development, and efforts to eradicate poverty* (pp. 3–24). Cambridge, UK: Cambridge University Press. https://doi.org/10.1017/9781009157940.001.

McKee, J. J., Rose, A. N., Bright, E. A., Huynh, T., & Bhaduri, B. L. (2015). Locally adaptive, spatially explicit projection of US population for 2030 and 2050. *Proceedings of the National Academy of Sciences*, *112*(5), 1344–1349. https://doi.org/10.1073/pnas.1405713112

Meijer, J. R., Huijbegts, M. A. J., Schotten, C. G. J., & Schipper, A. M. (2018). Global patterns of current and future road infrastructure. *Environmental Research Letters*, 13-064006. Data is available at www.globio.info.

Merkens, J. L., Reimann, L., Hinkel, J., & Vafeidis, A. T. (2016). Gridded population projections for the coastal zone under the Shared Socioeconomic pathways. *Global and Planetary Change*, *145*, 57–66. https://doi.org/10.1016/j.gloplacha.2016.08.009

Murakami, D., & Yamagata, Y. (2019). Estimation of gridded population and GDP scenarios with spatially explicit statistical downscaling. *Sustainability*, *11*(7), 2106. https://doi.org/10.3390/su11072106

Nam, K. M., & Reilly, J. M. (2013). City size distribution as a function of socioeconomic conditions: An eclectic approach to downscaling global population. *Urban Studies*, *50*(1), 208–225. https://doi.org/10.1177/0042098012448943

Narayanan, B., Aguiar, A., & McDougall, R. (2012). *Global Trade, assistance, and production: The GTAP 8 data base*. Center for Global Trade Analysis, Purdue University.

O'Neill, B. C., Kriegler, E., Ebi, K. L., Kemp-Benedict, E., Riahi, K., Rothman, D. S., van Ruijven, B. J., van Vuuren, D. P., Birkmann, J., Kok, K., Levy, M., & Solecki, W. (2015). The roads ahead: Narratives for shared socioeconomic pathways describing world futures in the 21st century. *Global Environmental Change*, *42*, 169–180. https://doi.org/10.1016/j.gloenvcha.2015.01.004

Organisation for Economic Co-operation and Development. Working Party on Territorial Indicators. (2012). *Redefining" urban": A New Way to Measure Metropolitan Areas*. OECD.

Parrado, R., & De Cian, E. (2014). Technology spillovers embodied in international trade: Intertemporal, regional and sectoral effects in a global CGE framework. *Energy Economics*, *41*(2014), 76–89. https://doi.org/10.1016/j.eneco.2013.10.016

Pinheiro, J., Bates, D., DebRoy, S., Sarkar, D., Heisterkamp, S., Van Willigen, B., & Maintainer, R. (2022). nlme: Linear and Nonlinear Mixed Effects Models. *R package version 3.1-158*. https://CRAN.Rproject.org/package=nlme

Reimann, L., Merkens, J. L., & Vafeidis, A. T. (2018). Regionalized Shared Socioeconomic Pathways: Narratives and spatial population projections for the Mediterranean coastal zone. *Regional Environmental Change*, *18*(1), 235–245. https://doi.org/10.1007/s10113-017-1189-2

Riahi, K., Van Vuuren, D. P., Kriegler, E., Edmonds, J., O'Neill, B. C., Fujimori, S., Bauer, N., Calvin, K., Dellink, R., Fricko, O., Lutz, W., Popp, A., Cuaresma, J. C., Samir, K. C., Leimbach, M., Jiang, L., Kram, T., Rao, S., Emmerling, J., Ebi, K., … Tavoni, M. (2017). The shared socioeconomic pathways and their energy, land use, and greenhouse gas emissions implications: An overview. *Global Environmental Change*, *42*, 153–168. https://doi.org/10.1016/j.gloenvcha.2016.05.009

Rohat, G. (2018). Projecting drivers of human vulnerability under the shared socioeconomic pathways. *International Journal of Environmental Research and Public Health*, *15*(3), 554. https://doi.org/10.3390/ijerph15030554

Rosenthal, S. S., & Strange, W. C. (2020). How close is close? The spatial reach of agglomeration economies. *Journal of Economic Perspectives*, 34(3), 27–49. https://doi.org/10.1257/jep.34.3.27

Swan, L. G., & Ugursal, V. I. (2009). Modeling of end-use energy consumption in the residential sector: A review of modeling techniques. *Renewable and Sustainable Energy Reviews*, *13*(8), 1819–1835. https://doi.org/10.1016/j.rser.2008.09.033

Thisse, J. F. (2018). Human capital and agglomeration economies in urban development. *The Developing Economies*, *56*(2), 117–139. https://doi.org/10.1111/deve.12167

van Vuuren, D. P., Edmonds, J., Kainuma, M., Riahi, K., Thomson, A., Hibbard, K., Hurtt, G. C., Kram, T., Krey, V., Lamarque, J.-F., Masui, T., Meinshausen, M., Nakicenovic, N., Smith, S. J., & Rose, S. K. (2011). The representative concentration pathways: An overview. *Climatic Change*, *109*(1), 5–31. https://doi.org/10.1007/s10584-011-0148-z

van Vuuren, D. P., Lucas, P. L., & Hilderink, H. (2007). Downscaling drivers of global environmental change: Enabling use of global SRES scenarios at the national and grid levels. *Global Environmental Change*, *17*(1), 114–130. https://doi.org/10.1016/j.gloenvcha.2006.04.004

Viguié, V., Hallegatte, S., & Rozenberg, J. (2014). Downscaling long term socioeconomic scenarios at city scale: A case study on Paris. *Technological Forecasting and Social Change*, *87*, 305–324. https://doi.org/10.1016/j.techfore.2013.12.028

Wang, T., & Sun, F. (2020). Spatially explicit global gross domestic product (GDP) data set consistent with the Shared Socioeconomic Pathways [Data set]. Zenodo. https://doi.org/10.5281/zenodo.4350027

West, B. T., Welch, K. B., & Galecki, A. T. (2014). *Linear mixed models: A practical guide using statistical software*. CRC Press.

Wilby, R. L., & Wigley, T. M. (1997). Downscaling general circulation model output: A review of methods and limitations. *Progress in Physical Geography*, *21*(4), 530–548. https://doi.org/10.1177/030913339702100403

Yamagata, Y., Murakami, D., & Seya, H. (2015). A comparison of grid-level residential electricity demand scenarios in Japan for 2050. *Applied Energy*, *158*, 255–262. https://doi.org/10.1016/j.apenergy.2015.08.079

Yamagata, Y., & Seya, H. (2019). *Spatial analysis using big data: Methods and urban applications*. Academic Press.